

A Potential Method for Enhanced Performance of Nimodipine by Spanlastic Nanovesicle with Tween 40 as Edge Activator

Hussein K. Alkufi¹   and Hanan J. Kassab^{*2}  

¹Department of Pharmacognosy, College of Pharmacy, University of Thi-Qar, 64001, Iraq

²Department of Pharmaceutics, College of Pharmacy, University of Baghdad, Baghdad, Iraq.

*Corresponding Author

Received 27/5/2024, Accepted 23/10/2024, Published 25/5/2025



This work is licensed under a Creative Commons Attribution 4.0 International License.

Abstract

By definition, spanlastic nanovesicles (SNVs) are small, solid, colloidal particles with a size range of 1 to 1000 nm, composed of edge activators (EAs) and nonionic surfactants. SNVs are intriguing options for drug administration and targeting, and they have garnered significant interest in a variety of sectors, including imaging and diagnostics. Nanovesicles' production and stability are critical to their effectiveness. Spanlastics are elastic vesicles that can encapsulate medications, enhancing their absorption and distribution. Nonionic surfactants help encapsulate hydrophilic and hydrophobic medications, improving their solubility. They usually have a hydrophilic (water-attracting) head and a hydrophobic (water-repelling) tail. The current work aims to improve the low solubility and dissolving rate of nimodipin (NMD) by formulating SNVs with nonionic surfactant, EAs, and soluplus as a stabilizer. We made them using the ethanol injection method, following a 3-level factorial design. The majority of the created NMD-SNVs formulations, according to the results, had particle sizes in the nanoscale range. The optimized formula (F19) had a polydispersity index (PDI) of 0.2905 and a particle size (PS) of 102.6 nm. In addition, it showed a higher rate of dissolution (86.91%) in phosphate buffer pH 7.2 with 1% Brij-35 in 8 hrs. as opposed to 51.33% for pure NMD in the same media at 12 hrs. with dialysis bag and higher release without dialysis bag, as well as improvement in entrapment efficiency (EE) and stability. When combined, NMD-SNVs greatly increased NMD's solubility and rate of dissolution, providing a promising nanoplatform for hydrophobic drug delivery.

Keywords: Edge activator, Non-ionic surfactant, Nimodipine, Spanlastic nanovesicle, Study design, Soluplus.

Introduction

Strokes are thought to be the leading cause of death after heart-related conditions. Acute subarachnoid hemorrhage (SAH), the cause of 1%–7% of strokes, is caused by ruptured brain aneurysms after trauma ⁽¹⁾. SAH causes 25–50% of fatalities and 50% of permanent disabilities, respectively ⁽²⁾. Vasospasm, the leading cause of disability in 70% of SAH patients, causes ischemia and death by obstructing the brain's ability to receive enough oxygen ⁽³⁾. NMD is a powerful drug that binds to fat and blocks the L-type calcium ion channel in 1,4-dihydropyridine. Its effects on cerebral artery dilation and cerebral blood flow augmentation make it the principal tool used in SAH management ⁽⁴⁾. The limited therapeutic efficacy of NMD stems from its susceptibility to first-pass metabolism, leading to low water solubility (3.86 µg/mL) and poor bioavailability (5–13%). For a duration of 21 days, NMD is taken orally every four hours. The oral dose is very high (360 mg/day) to compensate for its low bioavailability ⁽⁵⁾. Various approaches, such as the

production of solid lipid nanoparticles (SLNs) ⁽⁶⁾, NMD nanocrystals ⁽⁵⁾, NMD mixed micelles ⁽⁷⁾, mesoporous silica ⁽⁸⁾, and NMD pegylated nanoparticles ⁽⁹⁾, aim at preventing the hepatic first-pass effect and boosting NMD's oral bioavailability. Enhancing the bioavailability of NMD has been the successful outcome of most attempts to improve NMD's inadequate pharmacokinetic characteristics when delivered orally.

Nanovesicular systems like liposomes and niosomes, composed of polar and non-polar parts, have the ability to store both water-loving and fat-loving medicines. Research findings indicate that the encapsulation of NMD within nanovesicles enhances both its stability and bioavailability. However, these common carriers are neither flexible nor malleable as they travel across various cellular membranes ⁽¹⁰⁾. Therefore, recent studies have looked into ways to increase the deformability of these distinctive nanovesicles in order to increase their permeability through different

biological membranes ⁽¹¹⁾. Spanlastics are surfactant-dependent, malleable nanocarriers. Most spanlastics consist of EAs and non-ionic surfactants. EAs destabilize the nanocarriers' vesicular membranes by squeezing through various biological layer pores without breaking, increasing their permeability and flexibility across biological membranes ⁽¹²⁾.

Nanospanlastics are nanovesicles that are malleable, safe, and biodegradable. They also show greater chemical stability as compared to standard liposomes. Consequently, nanospanlastics serve as a stable nanocarrier that can hold NMD. Furthermore, spanlastics can improve NMD's penetration because they are flexible and can pass through tiny pores in biological membranes ⁽¹³⁾.

The goal of this work was to create NMD-loaded SNVs and study the effects of various parameters such as sonication time, polymer ratio, and stabilizer type on particle size, PDI, and EE% in order to maximize solubility and dissolving rate.

Materials and Methods

Materials

Nimodipine was purchased from Hyperchem in China. Ethanol was purchased from Honeywell International Inc., USA. Soluplus® was gifted from BASF, Germany. Span 60 and Tween

40 from Hyper Chem, China; Brij®-35 from Central Drug House, India. Dialysis bag 8-14 kDa Lab Pvt. Ltd., USA. Amicon ultrafilter with a MWCO 3 kDa. purchased from Sigma-Aldrich, Merck. All other chemicals were of analytical grade.

Model generation by three-level Factorial Design of NMD-Loaded SNVs

Using Design Expert 11 software (Stat-Ease, Inc., USA), 3-level factorial designs were built to assess the effects of three formulation components alone and in combination. The independent variables were the concentration of span 60: tween 40 (X1, ratio), the concentration of soluplus (X2, mg), and the duration of sonication (X3, minute). The three-component concentration weighed a total of 250 mg. Particle size (Y1), polydispersity index (PDI) (Y2), and entrapment efficiency (Y3) were the dependent variables (responses). Early research investigations served as the foundation for determining each factor's domain. Table 1 displays the response constraints, as well as the upper and lower bounds for the independent variables. The preparation of NM-loaded spanlastic nanovesicles at a concentration of 1.0 mg/mL involved maintaining a consistent amount of NMD.

Table 1. enumerates the variables and their corresponding values.

Variables	Levels		
	Low	middle	high
Independent variables			
X1	9:1(-1)	7:3(0)	5:5(1)
X2	0	25	50
X3	0	15	30

Preparation of SNVs formulations

Spanlastics were created utilizing the ethanol injection technique ⁽¹⁴⁾. In other words, NMD and span 60 were dissolved in 5 milliliters of pure ethanol. Warm tween 40 aqueous solution, either with or without soluplus (10 mL), was slowly injected with the alcoholic solution while being stirred at 1000 rpm and 60 °C using a magnetic stirrer. Following one hour of stirring, the resulting dispersion was bath-sonicated at various times to eliminate any aggregates, as shown in Table 2. Ultimately, the mixtures were refrigerated until further examination.

Characterization of NMD -SNVs

Particle size (PS) and polydispersity index (PDI)

A Malvern zetasizer particle size analyzer (Uitra Red, USA) model was used to determine the PS of all NMD-SNVs formulations at room temperature using a dynamic light scattering (DLS) technique. At a 90° scattering angle, the measurements were made. Distilled water was used to dilute the sample in a volume-to-volume ratio of 1:10. The previously mentioned technique measures the dispersion of particles moving in a

Brownian motion and then converts it into a dimension size distribution ⁽¹⁵⁾.

Encapsulation efficiency Evaluation

By centrifuging 4 milliliters of the dispersion at 3000 rpm for 15 minutes with an Amicon ultrafilter that had a molecular weight cut-off (MWCO) of 10 kDa, the %EE was ascertained. This process makes it possible to measure the amount of medication contained within the SNVs. By measuring the UV absorbance at a wavelength of 237 nm, spectrophotometry was used to determine the amount of unbound medication. Equation (1) was then used to calculate the quantity of drug trapped in the system ⁽¹⁶⁾.

$$EE\% = \frac{S-T}{S} \times 100 \quad (1)$$

T is the actual amount of free drug in each sample, and S is the total amount of drug that is theoretically present in the obtained sample.

Solubility determination

A volume (1.5 ml) of selected NMD-SNVs was dissolved in 2 ml of distilled water and shaken for 48 hrs. at room temperature in shaker water bath. Tubes were centrifuged, and the clear supernatant was filtered through a 0.45µ filter

syringe, properly diluted, and spectrophotometrically measured at 238 nm to be compared with pure NMD solubility. Triplicates of each experiment were conducted^(17,18).

Zeta potential measurement

The Malvern Zetasizer Nano ZS instrument (Malvern Instrument, Worcestershire, UK) was used to measure the electrophoretic mobility of a selected formula. The zeta potential, which measures the stability of the created dispersion and tells us about the level of repulsion between charged particles, was then calculated from this measurement. The specimen was placed into an electrophoretic cell by exposing the specimen to a 15.2 V/cm electrical field^(18,19).

Drug-excipient Compatibility for optimized formula

Studied via FTIR and DSC respectively, for optimized formula and compared with pure drug and physical mixture⁽²⁰⁾.

Field Emission-Scanning Electron Microscope (FE-SEM)

We examined the morphology of the optimized formula using a model from Inspect 50 FEI, Germany, at various magnifications. After being uniformly distributed onto double-sided carbon tapes using adhesive, the optimized formula specimens were fastened to FE-SEM specimen mounts. Prior to imaging, the samples were sputter-coated for two minutes to provide a uniform coating. The process involved applying a thin layer to the samples in order to increase conductivity and provide better imaging⁽²¹⁾.

In vitro drug release study

We conducted the release study using two methods. The first method is a membrane-free system, and the second method is a dialysis bag⁽²²⁾. The membrane dialysis technique was utilized to check the in vitro drug release from the optimized spanlastic formula. This was compared to the drug diffusion from its solution in pH 7.2 buffer with

1% brij-35. The drug solution and the optimized formulation equivalent to 3 mg of drug were taken for the diffusion study. Samples were added to a dialysis bag (MWCO 8000–14000 Da) that was pre-soaked with dissolution medium overnight, through which samples were placed inside. After that, the dialysis bags were loaded on the shafts of the beaker dissolution method⁽²³⁾. The rotation speed was set to be 100 rpm, and the temperature was 37 ± 0.1 °C. We used a buffer solution (pH 7.2, 300 mL) as the dissolution medium and added 1% Brij-35 to achieve sink conditions where the solubility of NMD in phosphate buffer (pH 7.2) equals 0.25. Samples (5 mL) were withdrawn during dissolution testing at the following time intervals: 0.5, 1, 1.5, 2, 3, 4, 6, 8 and 12 h. The drug concentrations were analyzed using a UV spectrophotometer at the predetermined λ_{max} (238 nm) (24). All experiments were done in triplicate, and the average values \pm standard deviations were recorded.

Statistical analysis

In order to identify significant differences among the relevant data, the experiment's results were reported as the mean and standard deviation (SD) of samples taken in triplicate using one-way analysis of variance (ANOVA). With the use of Design Expert 11 software, the result was deemed substantially different at a p-value of less than 0.05.

Results and Discussion

Analysis of the three-level Factorial Design of NMD-Loaded SNVs

The contents and evaluations (EEI%, PDI, and PS) of NMD-loaded nanospanlastic formulations made in line with the three-level factorial designs are shown in Table 2. By comparing the factor coefficients, regression equations showed how different independent variables affected the investigated responses.

Table 2. Three-level Factorial Design with measured responses

Run	X1	X2	X3	Y1	Y2	Y3
1	0	25	15	163.5	0.3916	88.55
2	0	25	0	215.1	0.3664	89.01
3	1	25	15	75.93	0.2949	76.09
4	-1	0	15	269.7	0.4283	90.76
5	0	50	0	134.2	0.2245	86.95
6	1	50	15	73.56	0.2915	75.87
7	1	0	15	93.41	0.3515	80.01
8	-1	0	0	551.3	0.4583	94.34
9	-1	25	0	226.1	0.3689	93.88
10	-1	50	15	165.3	0.2563	90.08
11	0	0	15	161.9	0.5016	86.99
12	1	0	30	81.99	0.5742	75.09
13	1	0	0	190.2	0.5286	83.55
14	1	25	0	108.3	0.2884	79.56
15	0	0	0	250.7	0.5063	89.23
16	-1	25	30	172.6	0.3593	88.56

17	1	50	0	75.55	0.2318	77.97
18	-1	50	0	207.1	0.2859	92.87
19	0	50	30	102.6	0.2905	84.55
20	0	0	30	155	0.4783	86.01
21	1	25	30	69.73	0.2178	74.76
22	-1	25	15	190.1	0.3399	91.65
23	-1	50	30	159.6	0.2568	87.55
24	1	50	30	65.1	0.2826	73.45
25	0	25	30	132.1	0.2526	86
26	0	50	15	104.7	0.2723	85.76
27	-1	0	30	363.9	0.4318	89.99

Figure 1's 3D response diagram displays the effects of the independent variables (X1:ratio of span 60 to tween 40), (X2: soluplus concentration), and (X3: sonication time) on dependent variables of NMD-SNVs formula (Y1:PS), (Y2:PDI), and (Y3:%EE).

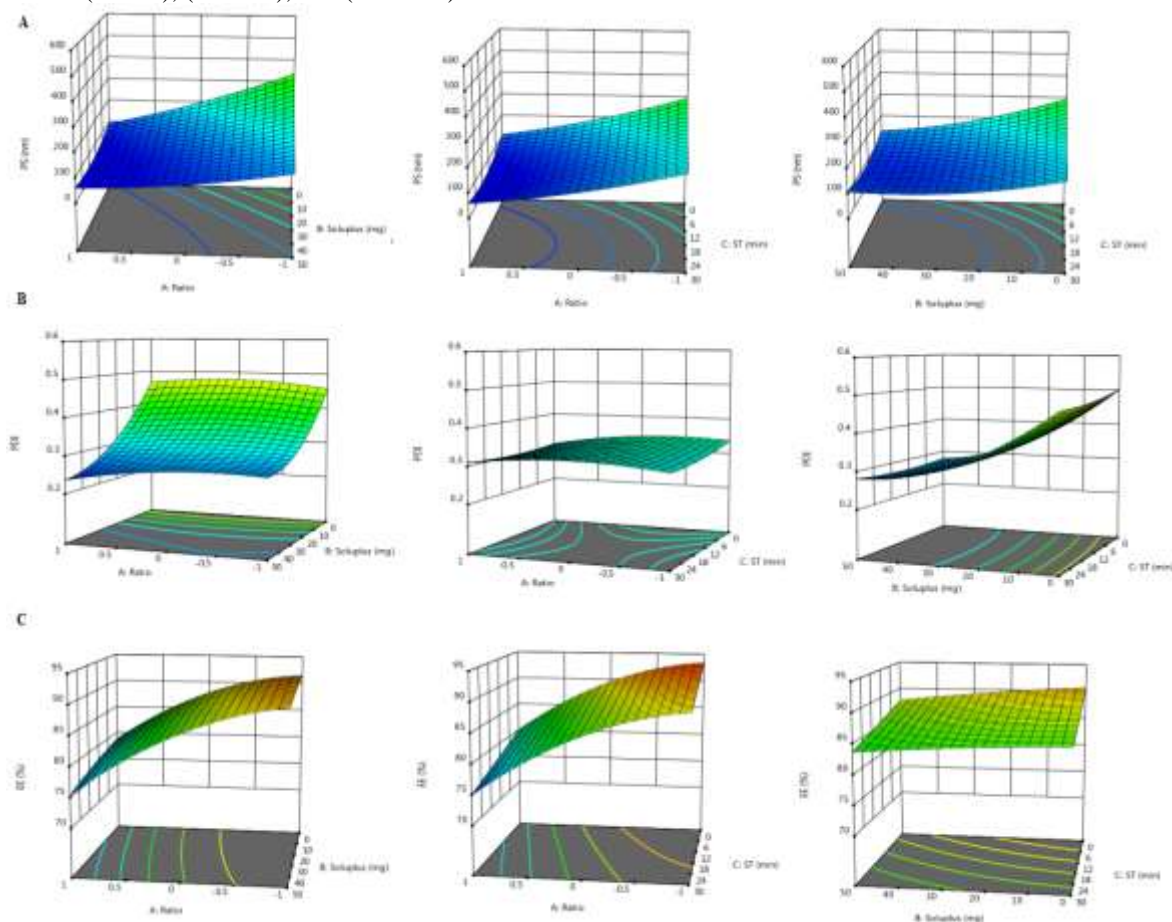


Figure 1. 3D-response charts express the effect of independent variables on (A) PS, (B) PDI, and (C) EE%

Effect of Independent Variables on PS

According to the particle size investigation's findings (Table 2), several pieces of spanlastic had sizes ranging from 10 to 100 nm. However, when compared to NMD-loaded SNVs without soluplus (551.3 ± 2.53 nm to 81.99 ± 2.06 nm), the particle sizes of NMD-loaded SNVs with a high concentration of soluplus (50 mg/10 ml) showed significantly ($p < 0.05$) lower particle sizes (207.1 ± 4.08 nm to 65.1 ± 3.21 nm). The spanlastic formulation with Soluplus had small particles ($p < 0.05$) compared to the spanlastic without Soluplus, as shown in Table 3.

The sonication cycle performed after the drug was loaded may have helped reduce the size of the vesicles⁽²⁵⁾. The inclusion of Soluplus had the capacity to influence the size of the spanlastic vesicles. A recent report demonstrated Soluplus's ability to spontaneously self-assemble into spherical particles, with most of the resulting particle sizes less than 50 nm⁽²⁶⁾. Additionally, PEG 6000, which is a component of Soluplus's structure, has a tendency to form strong or tightly bound bilayers, which can lead to a decrease in vesicle size⁽²⁷⁾.

Table 3. Summary of ANOVA for the PS response parameters

Source	Sum of Squares	df	Mean Square	F-value	p-value	
Model	2.033E+05	3	67750.47	19.22	< 0.05	Significant
X1	1.204E+05	1	1.204E+05	34.15	< 0.0001	Significant
X2	58983.53	1	58983.53	16.73	0.0004	Significant
X3	23902.45	1	23902.45	6.78	0.0159	Significant

Effect of independent variables on PDI

The PDI ranged from 0.5742±0.004 to 0.2178±0.004. The polydispersity index can be used to determine whether a sample is more heterogeneous or more homogeneous. Its purpose is to specify how uniform or nonuniform a particle size distribution is. Less than 0.5 for the polydispersity index (PDI) indicates monodispersed particles. For a sample with perfectly uniform particle size, the PDI's numerical value ranges from 0.0 to 1.0; for a highly polydisperse sample with multiple particle size populations, the range is 1.0 to 0.0. A value greater than 0.7 indicates a polydispersed or widely distributed particle size distribution in the sample ⁽²⁸⁾. The population of

spanlastic vesicles is homogeneous when the PDI is 0.3 or less; the spanlastic vesicle population is uniform. The results showed that only the batch formula had a PDI greater than 0.3; this could be because Soluplus was not present. As indicated in tables 2, 3, and 4, the stabilizing effect of the Soluplus formula yielded narrower PDI and significantly reduced particle sizes ($p < 0.05$) when compared to the absence of the Soluplus method. Additionally, compared to the batch without Soluplus, it was shown that the presence of Soluplus had a substantial impact on the PS of the spanlastic, resulting in much smaller diameters ($p < 0.05$) with a narrow PDI ($p < 0.05$) ⁽²⁹⁾.

Table 4. Summary of ANOVA for the PDI response parameters

Source	Sum of Squares	df	Mean Square	F-value	p-value	
Model	0.2151	3	0.0239	6.72	< 0.05	Significant
X1	0.0009	1	0.0009	0.2410	0.6298	No significant
X2	0.1936	1	0.1936	54.43	< 0.0001	Significant
X3	0.0007	1	0.0007	0.2073	0.6546	No significant

Effect of Independent Variables on EE%

Studies have indicated that the efficacy of entrapment rises as the Span60 content does; still, optimal Span60 concentration is necessary for effective entrapment and vesicle formation. At ratios of low Tween40 content (9:1) the particle size increased therefore the EE improved, but when a 7:3 ratio of (Span60: Tween 40) the particle size decreased with very acceptable entrapment, and the net average curvature of Span 60 (hydrophobic surfactant) allowed the formation of vesicles, which affected the drug entrapment.

The situation is different for batch 1 ratio, which had the highest tween40 content (125 mg) but the least amount of entrapment, indicating an

insufficient span60 ratio that increases fluidity of the system and has a negative impact on entrapment efficiency. This is evident in the batch 1 ratio formulation, which produced an entrapment of less than 70%. In order to create spanlastic with increased drug encapsulation, nonionic surfactants with long hydrocarbon chains and a small hydrophilic head area were used ⁽³⁰⁾.

It was evident that batches 9:1 and 7:3 ratios for the NMD-loaded SNVs had noticeably higher EE ($p < 0.05$) than batch 5:5 ratios. Even though it is thought to increase the integrity of the vesicles produced, adding Soluplus to the formulation process decreases entrapment, but not significantly ($p > 0.05$), as indicated in Table 5.

Table 5. Summary of ANOVA for the EE response parameters

Source	Sum of Squares	df	Mean Square	F-value	p-value	
Model	1017.18	3	113.02	96.65	< 0.05	Significant
X1	845.02	1	845.02	722.63	< 0.0001	Significant
X2	3.82	1	3.82	3.27	0.0884	No significant
X3	95.22	1	95.22	81.43	< 0.0001	Significant

Optimization of NMD-SNVs formulas

Optimization is the process of using systematic methods to obtain the optimal combinations needed to manufacture a superior-quality pharmaceutical formula. It entails determining the optimal formula by first examining the impact of various independent factors on

pharmaceutical formulations' properties. The optimization procedure sought to reduce PS, increase EE%, and minimize PDI. According to the findings, F19 had the greatest desirability score. Furthermore, for Y1, Y2, and Y3, the projected values of F19 were 102.6 nm (Figure 3), 0.2905, and 84.55%, respectively.

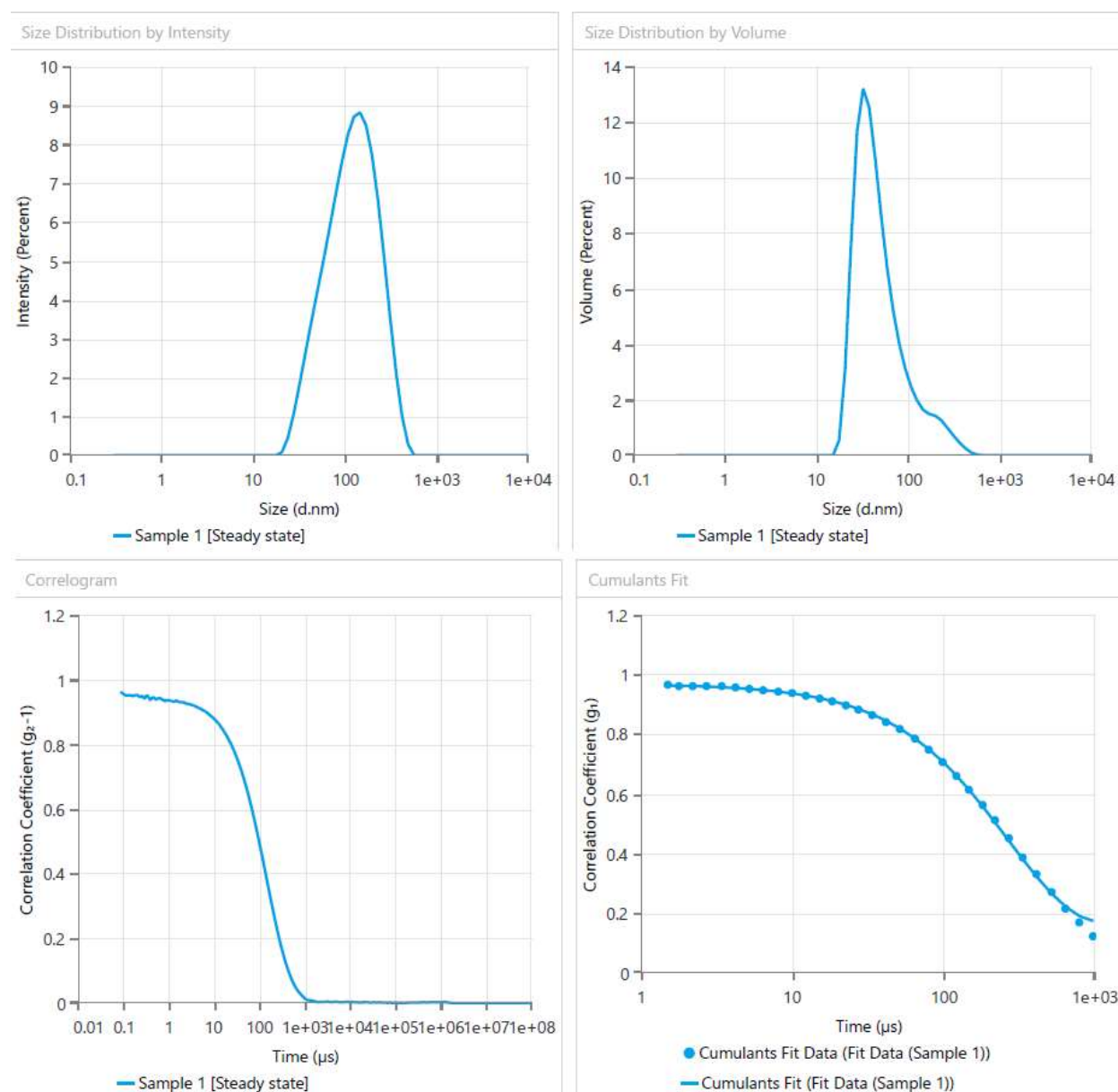


Figure 2. Average PS for optimum formula F19 by Malvern zeta seizer according to intensity of PS

Solubilization capacity of SNVs

The solubility study's goal was to identify the variables influencing NMD solubility in order to improve the medication payload and broaden the application of SNVs formulations. The pure medication has a solubility of 0.01 mg/ml, making it nearly practically insoluble in water with 1%Brij-35. NMD-SNVs have a solubility value of 2.31 mg/ml, making them somewhat soluble in water with 1%Brij-35. The increased surface area-to-

volume ratio of nanovesicles enables more interaction with the solvent. Improved solubility may result from the drug's faster rate of dissolution due to its larger surface area ⁽⁴⁾.

Zeta potential (ZP)

For optimized formula (F19) was found (-28.08 ± 1.01) mV confirming that there would be no instability issues with the developed formulation as shown in Figure 3.

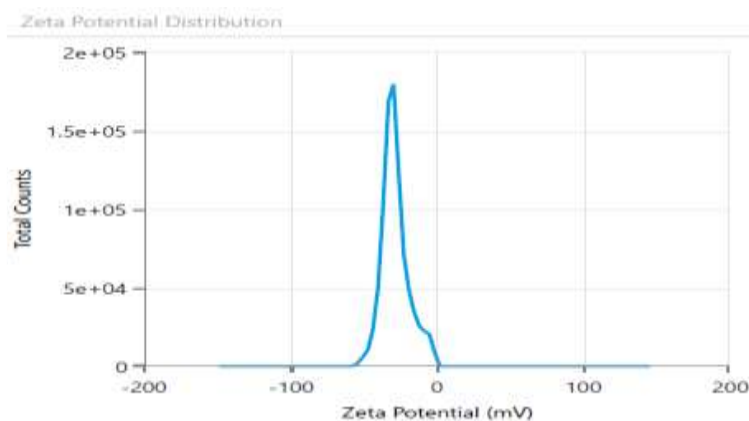


Figure 3. Average zeta potential distribution.

Field Emission-Scanning Electron Microscope (FE-SEM)

undertook the research on optimal (F19) morphologies. The NMD-SNVs (F19) analysis

revealed that the NMD particles were integrated into the vesicles and had a shape that was almost spherical in the nanoscale size range between 10 and 100 nm (Figure 4)⁽³¹⁾.

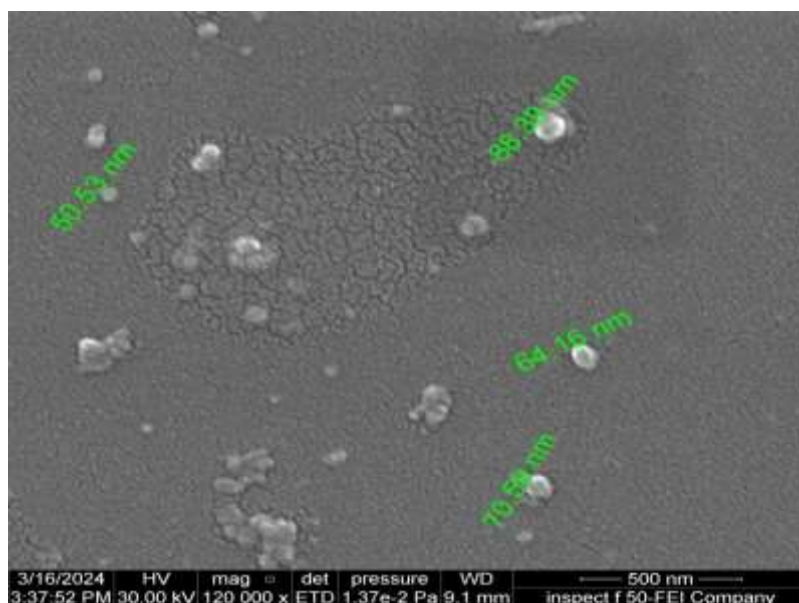


Figure 4. FE-SEM of NMD-SNVs (F19)

Compatibility Study

Figure 5(a) shows the DSC thermograms of the pure NMD exhibited a sharp endothermic peak at 125.78 °C, which is in line with its melting crystallinity⁽⁴⁾.

Figure 5(b) shows the DSC thermograms of the physical combination exhibited a sharp endothermic peak at 51.13 °C. The use of a high concentration of span60 with NMD can indeed lead to the disappearance of the NMD peak in DSC.

This is primarily due to matrix effects and amorphization⁽¹⁸⁾.

Figure 5(c) shows the DSC thermograms of the optimized (F19) lyophilized NMD-SNV powder exhibiting a sharp endothermic peak at 155.36 °C, indicating that the solubilizing action of surfactants was responsible for trapping the NMD inside the SNVs, and mannitol's osmotic effects can lead to the dehydration of the drug, which, in turn, can cause the disappearance of the drug's peak in DSC⁽³²⁾.

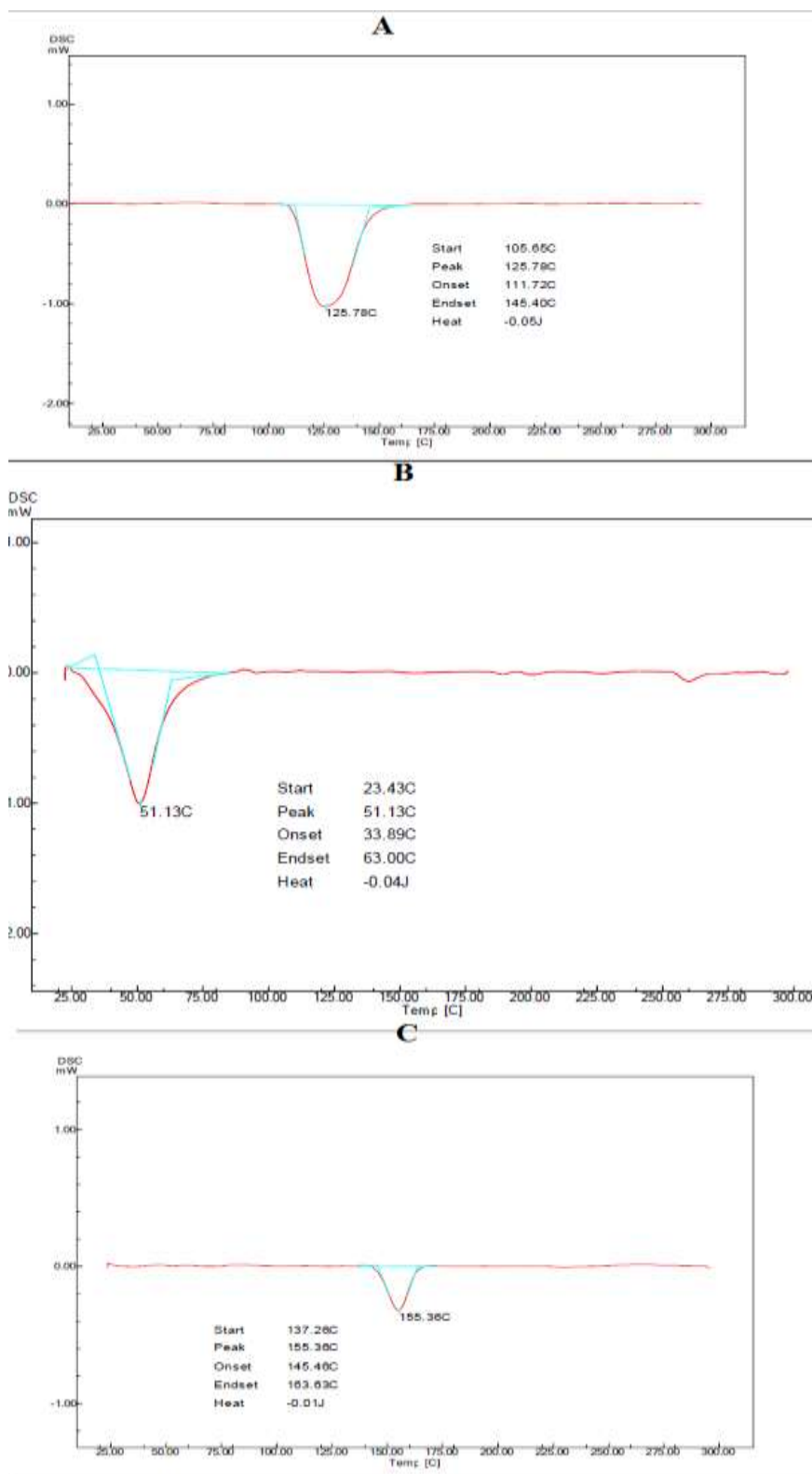


Figure 5. DSC thermogram of a) pure NMD, b) physical mixture, and c) lyophilized F19

As seen in Figure 6, the drug-excipient compatibility was investigated using FTIR for pure NMD, physical mixtures, and optimized F19. Characteristic peaks in the pure NMD spectra are (3088 cm^{-1}) and (3273 cm^{-1}) NH stretching. C-H aliphatic and aromatic stretching (2943 cm^{-1}). -C-CH₃(1381 cm^{-1}), aromatic C=C stretching (1622

cm^{-1}), pyridine NH(1641.84 cm^{-1}), carbonyl stretching of ester (1699 cm^{-1}), NO₂ stretching ($1531, 1303.43\text{ cm}^{-1}$), and C-H bending (1130 cm^{-1})⁽²⁾.

However, the formation of hydrogen bonds between the hydrophilic groups present on excipients such as soluplus, span 60, and NMD

caused the peaks of C=O and NO₂ to shift and lose intensity. The formulation's spectra revealed a broad peak of approximately 3273 cm⁻¹. In conclusion, the investigation showed that there are

no recognized chemical interactions, leading us to believe that the creation of hydrogen bonds is what is responsible for the medication's increased solubility⁽⁴⁾.

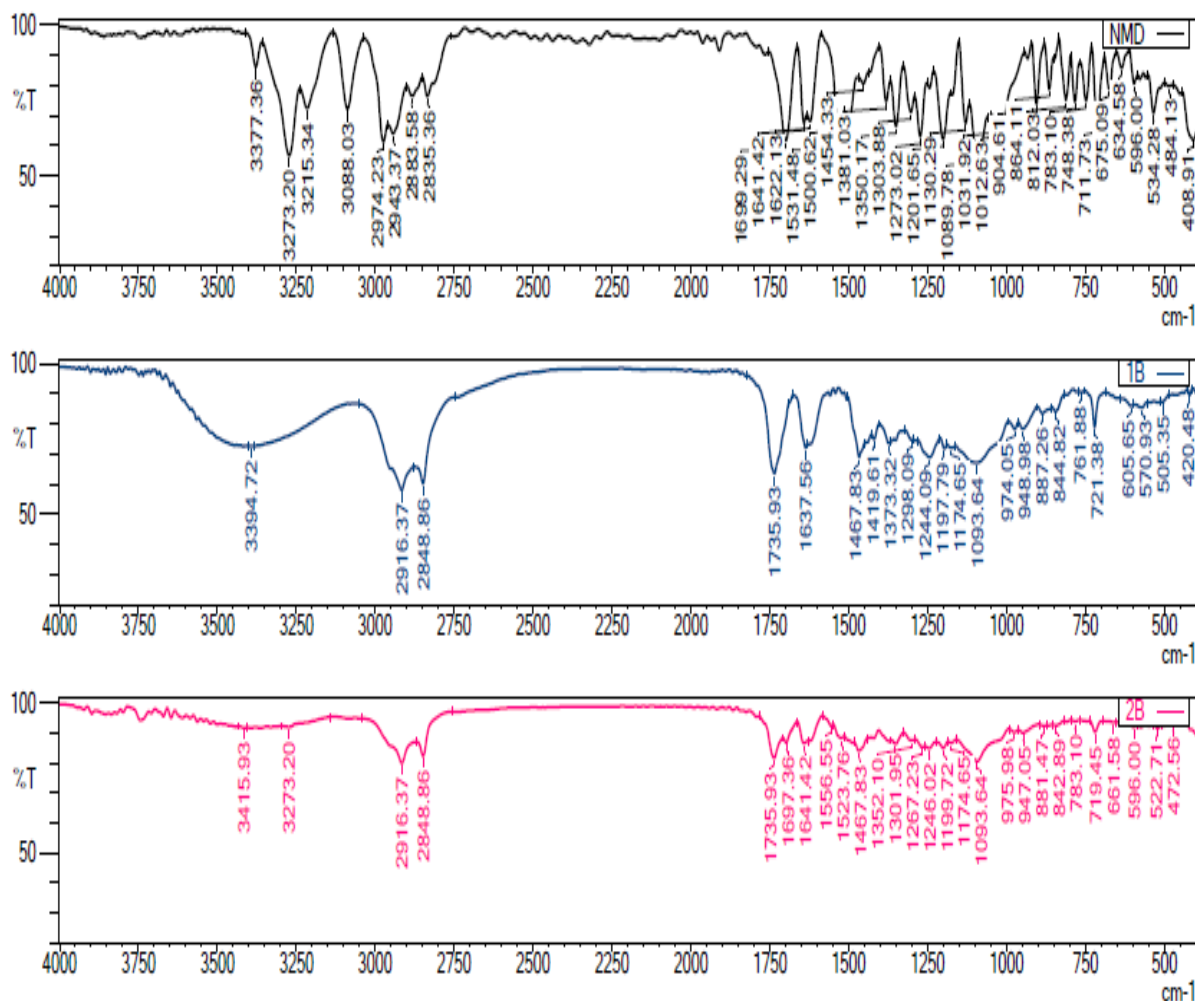


Figure 6. FTIR of NMD,(1B) physical mixture and (2B) optimum formula (F19)

In-vitro Drug diffusion study — comparison of test methods

Figure 7 compares the percentages of NMD release from SNVs-F19 dispersions obtained by two different methods. The results indicate clear differences between the methods for both pure NMD. In the first method without a dialysis membrane, a rapid release of a significant fraction of the active substance (100%) was observed already within 10 min of the study, while the pure drug achieved a large percent at 60 min, equal to 30.42%. As shown in Figure 7(A), the NMD-SNVs formulation exhibits burst release in the first method. Significantly different release profiles were obtained in second methods with dialysis membranes. Primarily, there was no burst effect and showed a much higher and more sustained release of 86.91% within 8 hours than the pure drug, which obtained a release of 51.33% in the same media within 12 hr, as shown in Figure 7 (B) (33-35). Due to numerous factors that can be modified

and have a significant impact on the result of *in vitro/in vivo* correlation. The discrepancy in release rates between the two *in vitro* dissolution methods is likely due to the dialysis membrane's permeability. The first approach Without a dialysis membrane, the drug molecules have direct and unrestricted access to the dissolution medium. This allows for rapid diffusion of the drug into the solution, leading to a rapid release profile. The second method with the dialysis membrane acts as a barrier between the drug and the dissolution medium. The membrane's pore size determines the rate at which drug molecules can pass through. The pore size is small, so the drug molecules will have to diffuse through the membrane, which is a slower process than direct diffusion. This results in a sustained release profile where the drug is gradually released over time. As well, the efficiency of SNVs technique was demonstrated by comparing the diffusion profile of f19 with pure NMD, as shown in figure 7. The profile showed

that the diffusion rate in the two methods of NMD in SNVs was higher as compared to that of pure NMD. The similarity factor f_2 was found to be the difference between SNVs and pure drugs according to f_2 in the first and second methods, which equal 5.69 and 26.77, respectively ⁽³⁶⁾.

In summary, the use of a dialysis membrane in the second method creates a controlled release system that slows down the drug release rate compared to the method without dialysis.

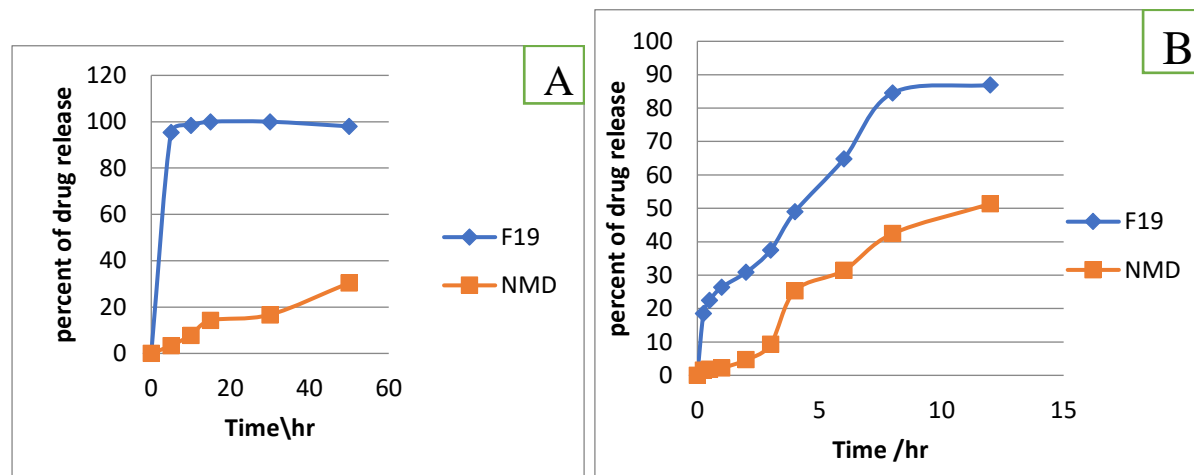


Figure 7. Pure NID and NMD-SNVs (F19) in BPS pH 7.2 with 1% Brij-35: Figure 7 shows the in vitro drug release investigation (A) without a dialysis bag and (B) with a dialysis bag.

Conclusion

The findings showed that adding solupus to NMD-SNVs is a possible way to make very strong, stable, and soluble nanoscale systems with better properties and controlled release behavior. The ethanol injection method was more effective in producing tiny PS with a comparatively high entrapment efficiency. The polymer ratio and sonication time, as well as the stabilizer concentration, all are impacted by the size of the nanovesicles.

Acknowledgment

The information used in this study was taken from a doctoral thesis that was submitted to the University of Baghdad's College of Pharmacy's Committee on Graduate Studies, as well as the Department of Pharmaceutics. The writers express their sincere gratitude to the University of Baghdad's College of Pharmacy for their invaluable assistance in providing the resources and instruction necessary to make this work possible.

Conflicts of Interest

The authors declare that there is no conflict of interest

Funding

This research did not receive any specific fund

Ethics Statements

This study was in vitro and does not need ethical approval from an ethics committee.

Author Contribution

H.K.A. Data collection, Investigation, Methodology, Writing –Original Draft Preparation. H.J.K. Project Administration, Supervision,

Writing –Review and approve the final version of the manuscript.

References

1. Feigin VL, Rinkel GJE, Lawes CMM, Algra A, Bennett DA, van Gijn J, et al. Risk factors for subarachnoid hemorrhage: an updated systematic review of epidemiological studies. *Stroke*. 2005;36(12):2773–80.
2. Ghareeb MM, Neamah AJ. Formulation and characterization of nimodipine nanoemulsion as ampoule for oral route. *Int J Pharm Sci Res*. 2017;8(2):591.
3. Al-Jehani H, Angle M, Marcoux J, Teitelbaum J. Early abnormal transient hyperemic response test can predict delayed ischemic neurologic deficit in subarachnoid hemorrhage. *Crit Ultrasound J*. 2018 Jan;10(1):1-6.
4. Alhagiesia AW, Ghareeb MM. Formulation and evaluation of nimodipine nanoparticles incorporated within orodispersible tablets. *Int J Drug Deliv Technol*. 2020;10(4):547–52.
5. Fu Q, Sun J, Zhang D, Li M, Wang Y, Ling G, et al. Nimodipine nanocrystals for oral bioavailability improvement: preparation, characterization and pharmacokinetic studies. *Colloids Surf B Biointerfaces*. 2013 Sep;109:161–6.
6. Chalikwar SS, Belgamwar VS, Talele VR, Surana SJ, Patil MU. Formulation and evaluation of Nimodipine-loaded solid lipid nanoparticles delivered via lymphatic transport system. *Colloids Surf B Biointerfaces*. 2012;97:109–16.
7. Basalious EB, Shamma RN. Novel self-assembled nano-tubular mixed micelles of

- Pluronics P123, Pluronic F127 and phosphatidylcholine for oral delivery of nimodipine: In vitro characterization, ex vivo transport and in vivo pharmacokinetic studies. *Int J Pharm.* 2015;493(1–2):347–56.
8. Li H, Li H, Wei C, Ke J, Li J, Xu L, et al. Biomimetic synthesis and evaluation of histidine-derivative templated chiral mesoporous silica for improved oral delivery of the poorly water-soluble drug, nimodipine. *Eur J Pharm Sci Off J Eur Fed Pharm Sci.* 2018;117:321–30.
 9. Moreno LCGEI, Solas M, Martínez-Ohárriz MC, Muñoz E, Santos-Magalhães NS, Ramirez MJ, et al. Pegylated nanoparticles for the oral delivery of nimodipine: Pharmacokinetics and effect on the anxiety and cognition in mice. *Int J Pharm.* 2018;543(1–2):245–56.
 10. Badria F, Mazyed E. Formulation of Nanospanlastics as a Promising Approach for Improving the Topical Delivery of a Natural Leukotriene Inhibitor (3-Acetyl-11-Keto- β -Boswellic Acid): Statistical Optimization, in vitro Characterization, and ex vivo Permeation Study. *Drug Des Devel Ther.* 2020;14:3697–721.
 11. Al-Mahallawi AM, Khowessah OM, Shoukri RA. Enhanced non invasive trans-tympanic delivery of ciprofloxacin through encapsulation into nano-spanlastic vesicles: Fabrication, in-vitro characterization, and comparative ex-vivo permeation studies. *Int J Pharm.* 2017;522(1–2):157–64.
 12. Zheng W, Fang X, Wang L, Zhang Y. Preparation and quality assessment of itraconazole transfersomes. *Int J Pharm.* 2012;436(1–2):291–8.
 13. Pandey M, Choudhury H, Gorain B, Tiong SQ, Wong GYS, Chan KX, et al. Site-Specific Vesicular Drug Delivery System for Skin Cancer: A Novel Approach for Targeting. *Gels* (Basel, Switzerland). 2021 Nov;7(4) 218. <https://doi.org/10.3390/gels7040218>
 14. Alhammid SNA, Kassab HJ, Hussein LS, Haiss MA. Spanlastics Nanovesicles: An Emerging and Innovative Approach for Drug Delivery. *Maaen J Med Sci.* 2023;2(2) 100-107.
 15. Abdelrahman FE, Elsayed I, Gad MK, Elshafeey AH, Mohamed MI. Response surface optimization, Ex vivo and In vivo investigation of nasal spanlastics for bioavailability enhancement and brain targeting of risperidone. *Int J Pharm.* 2017;530(1–2):1–11.
 16. Rashid AM, Abdal-Hammid SN. Formulation and characterization of itraconazole as nanosuspension dosage form for enhancement of solubility. *Iraqi J Pharm Sci.* 2019;28(2):124–33.
 17. Ghareeb MM. Formulation and characterization of isradipine as oral nanoemulsion. *Iraqi J Pharm Sci.* 2020;29(1):143–53.
 18. Salih OS, Al-Akkam EJ. Preparation, In-vitro, and Ex-vivo Evaluation of Ondansetron Loaded Invasomes for Transdermal Delivery. *Iraqi Journal of Pharmaceutical Sciences.* 2023 Dec 30;32(3):71-84.
 19. Jakubowska E, Milanowski B, Lulek J. A systematic approach to the development of cilostazol nanosuspension by liquid antisolvent precipitation (LASP) and its combination with ultrasound. *Int J Mol Sci.* 2021;22(22):12406.
 20. Guan T, Miao Y, Xu L, Yang S, Wang J, He H, et al. Injectable nimodipine-loaded nanoliposomes: preparation, lyophilization and characteristics. *Int J Pharm.* 2011;410(1–2):180–7.
 21. Gorajana A, Rajendran A, Rao NK. Preparation and in vitro evaluation of solid dispersions of nimodipine using PEG 4000 and PVP K30. *Asian Journal of Pharmaceutical Research and Health Care.* 2010;2(2):163-9.
 22. Wolska E, Szymańska M. Comparison of the In Vitro Drug Release Methods for the Selection of Test Conditions to Characterize Solid Lipid Microparticles. *Pharmaceutics.* 2023; 3;15(2):511.
 23. Corrigan OI, Timoney RF. Towards standardizing agitation conditions in the beaker dissolution method. *International Journal of Pharmaceutics.* 1978 ; 1;1(5):299-302.
 24. Alhagiesia AW, Ghareeb MM. The Formulation and Characterization of Nimodipine Nanoparticles for the Enhancement of solubility and dissolution rate. *Iraqi J Pharm Sci.* 2021;30(2):143–52.
 25. Chen XT, Wang T. Preparation and characterization of atrazine-loaded biodegradable PLGA nanospheres. *Journal of Integrative Agriculture.* 2019; 1;18(5):1035-41.
 26. Praveen A, Aqil M, Imam SS, Ahad A, Moolakkadath T, Ahmad FJ. Lamotrigine encapsulated intra-nasal nanoliposome formulation for epilepsy treatment: Formulation design, characterization and nasal toxicity study. *Colloids Surf B Biointerfaces.* 2019;174:553–62.
 27. Jassem NA, Abd Alhammid SN. Enhancement of the Dissolution and Solubility of Canagliflozin Using Nanodispersion Systems. *Al-Rafidain J Med Sci.* 2024;6(1):222–31.
 28. Muhammed SA, Al-Kinani KK. Formulation and in vitro evaluation of meloxicam as a self-microemulsifying drug delivery system. *F1000Res.* 2023 May 30;12:315. doi: 10.12688/f1000research.130749.2.
 29. Ugorji OL, Okoye OI, Nwangwu C, Agbo CP, Kenekwaku FC. Soluplus-stabilized 5-fluorouracil-entrapped niosomal formulations

- prepared via active and passive loading techniques: comparative physico-chemical evaluation. *Journal of Dispersion Science and Technology*. 2024;45(5):891-9.
30. Kenekukwu FC, Kalu CF, Momoh MA, Onah IA, Attama AA, Okore VC. Novel Bos indicus fat-based nanoparticulate lipospheres of miconazole nitrate as enhanced mucoadhesive therapy for oral candidiasis. *Biointerface Res Appl Chem*. 2022;13(1):24.
 31. Havrdova M, Polakova K, Skopalik J, Vujtek M, Mokdad A, Homolkova M, Tucek J, Nebesarova J, Zboril R. Field emission scanning electron microscopy (FE-SEM) as an approach for nanoparticle detection inside cells. *Micron*. 2014; 1;67:149-54.
 32. Taymouri S, Varshosaz J. Effect of different types of surfactants on the physical properties and stability of carvedilol nano-niosomes. *Adv Biomed Res*. 2016;5(1):48.
 33. Kang JH, Kim YJ, Yang MS, Shin DH, Kim DW, Park IY, Park CW. Co-Spray Dried Nafamostat Mesylate with Lecithin and Mannitol as Respirable Microparticles for Targeted Pulmonary Delivery: Pharmacokinetics and Lung Distribution in Rats. *Pharmaceutics*. 2021; 19;13(9):1519. doi: 10.3390/pharmaceutics13091519.
 34. Kassab HJ, Alkufi HK, Hussein LS. Use of factorial design in formulation and evaluation of intrarectal in situ gel of sumatriptan. *J Adv Pharm Technol Res*. 2023;14(2):119.
 35. Taher SS, Sadeq ZA, Al-Kinani KK, Alwan ZS. solid lipid nanoparticles as a promising approach for delivery of anticancer agents. *Mil Med Sci Lett Zdr List*. 2022;91(3).
 36. Hussein LS, Al-Khedairy EB. Solubility and dissolution enhancement of ebastine by surface solid dispersion technique. *Iraqi Journal of Pharmaceutical Sciences*. 2021; 30(1):122-32.

طريقة محتملة لتعزيز إداء عقار النيموديبيين باستخدام الحويصلات النانوية المرنة مع منشط العبور (توين ٤٠)

حسين كاظم الكوفي^١ و حنان جلال كساب^٢

^١ فرع العقاقير الطبية ، كلية الصيدلة ، جامعة ذي قار ، ذي قار ، العراق

^٢ فرع الصيدلانيات، كلية الصيدلة ، جامعة بغداد، بغداد ، العراق

الخلاصة

الحويصلات النانوية السبانلاستيك جزيئات غروية صغيرة صلبة ذات حجم يتراوح بين ١ و ١٠٠٠ نانومتر، تتكون من مُنَشِّط الحافة والمُستحلب غير أيوني. وتُعتبر الحويصلات النانوية السبانلاستيك خيارات مثيرة للاهتمام لإدارة وتوجيه الأدوية، وقد اجتذبت اهتمامًا كبيرًا في عدد من القطاعات، بما في ذلك التصوير والتشخيص. يعد إنتاج الحويصلات النانوية واستقرارها أمرًا أساسيًا لاستخدامها الفعال. تُعد السبانلاستيك حويصلات مرنة قادرة على تغليف الأدوية، مما يعزز امتصاصها وتوزيعها. تساعد المُستحلبات غير الأيونية على تغليف الأدوية المحبة للماء والغير محبة للماء، مما يحسن انحلالها. عادة ما يكون لها رأس محب للماء (يجذب الماء) وذيل غير محب للماء (يطرد الماء). يهدف العمل الحالي إلى تحسين انحلالية النيموديبيين المنخفضة ومعدل ذوبانه من خلال صياغة الحويصلات النانوية المرنة باستخدام مُستحلب غير أيوني، مُنَشِّطات الحافة، وسولوبليس كُثِّتَت. قمنا بإعدادها باستخدام طريقة حقن الإيثانول وفقًا لتصميم عاملي من ٣ مستويات. وفقًا للنتائج، كان لدى معظم صيغ الفورمولا المختارة أحجام جزيئات في النطاق النانومتري. وكانت الصيغة المحسنة لها مؤشر تشتت قدره ٠,٢٩٠٥، وحجم جزيئات قدره ١٠٢,٦ نانومتر. بالإضافة إلى ذلك، أظهرت معدلًا أعلى للانحلال (٨٦,٩١٪) في محلول فوسفات عازل بدرجة حموضة ٧,٢ مع ١٪ من بروج-٣٥ في ٨ ساعات مقارنة بـ ٥١,٣٣٪ للدواء في نفس الوسط في ١٢ ساعة مع كيس الديلزة وإطلاقًا أعلى بدون كيس الديلزة، فضلًا عن تحسين كفاءة التحمل والاستقرار. الصيغة المحسنة زادت بشكل كبير انحلالية النيموديبيين ومعدل ذوبانه، مما قدم منصة نانوية واعدة لتوصيل الأدوية الكارهة للماء

الكلمات المفتاحية: مُنَشِّط الحافة، مُستحلب غير أيوني، نيموديبيين، حويصلة نانوية سبانلاستيك، تصميم الدراسة، سولوبليس